Chapter 6
Long Term Analysis of Meteorological-Oceanographic Extreme Events for the Baixada Santista Region

Celia Regina de Gouveia Souza, Agenor Pereira Souza, and Joseph Harari

Abstract This chapter presents a database of extreme events, including storm surges (SS) and coastal inundation/flooding (CI/F) that caused injuries and economic/environmental losses in cities from Baixada Santista Metropolitan Region between 1928 and 2016 (hemerographic method). A group of seven indicators describes the boundary conditions of each event: duration/evolution interval, lunar phase, meteorological tide height, precipitation, wind direction and intensity, significant wave height and direction, and ENSO phases. They were listed 115 SS (76.5% only in the current century) and 123 CI/F (47.2%). Around 76.5% of SS occurred between April and September, while 50.4% of CI/F between January and April. Spring tides influenced 52.2% of SS and 65.6% of CI/F. Accumulated rainfall volume during the duration interval was 227.1 mm in SS and 277.8 mm in CI/F. Maximum height of meteorological tides was 0.78 m for both types. Wind intensity reached 20.6 m/s in SS and 17 m/s in CI/F events, both with predominant SW-SSW directions. Significant waves reached 7 and 5.5 m respectively in SS and CI/F, being S-SSE directions predominant. ENSO phenomenon seems to control these extreme events, once 54.8% of SS and 46.3% of CI/F occurred during EN, and 40% of SS and 37.4% of CI/F during LN phases.

Keywords Storm surge · Coastal inundation · Flooding · Boundary conditions · Long-term series

C. R. G. Souza (✉)
Institute of Geology – Secretariat for the Environment of the State of São Paulo (IG-SMA/SP), São Paulo, SP, Brazil

Post-Graduate Programme on Physical Geography – Faculty of Philosophy, Languages and Human Sciences, University of São Paulo (FFLCH-USP), São Paulo, SP, Brazil
e-mail: celia@sp.gov.br

A. P. Souza
Environmental consultant, São Paulo, São Paulo, Brasil

J. Harari
Institute of Oceanography, University of São Paulo, São Paulo, São Paulo, Brasil
e-mail: joharari@usp.br

L. H. Nunes et al. (eds.), *Climate Change in Santos Brazil: Projections, Impacts and Adaptation Options*, https://doi.org/10.1007/978-3-319-96535-2_6

6.1 Introduction

Coastal zones are influenced by oceanographic, atmospheric and continental processes and are therefore particularly sensitive to climate variations. In a climatic change scenario, sea-level rise and changes in the intensity, spatial distribution and temporal frequency of extreme meteorological-oceanographic events induced by wind, rain, waves and tides might produce significant impacts in these regions.

Much evidence suggest that climate changes have already modified the magnitude and frequency of extreme meteorological events around the world, though attributing isolated events to climate change is still difficult (IPCC 2012). Moreover, a general increase in extreme events is expected in future decades (IPCC 2014).

Brazil's coastal zone is very susceptible, and its inhabitants vulnerable, to climate change and its effects (Marengo et al. 2017a, b). Considering sea-level rise (SLR) alone, the consequences can be diverse, as they impact both natural and anthropogenic environments. In this regard, many Brazilian regions are already being affected by severe coastal erosion and coastal inundation linked to extreme storm and tidal surges (Souza et al. 2005; Muehe 2006; Nicholls 2006; Gasparro et al. 2008; Souza 2009a, b, 2010, 2011, 2012; Magrin et al. 2014; PBMC 2014; Marengo et al. 2017a, b).

A 61-year time span (1948–2008) of wave climate data reanalysis for the Latin American and Caribbean regions showed that many changes in wave height and the mean direction of the energy flux have occurred along the Brazilian coast, mainly in the South Region (Losada et al. 2013; Reguero et al. 2013; CEPAL 2016).

Reguero et al. (2013) and CEPAL (2016) pointed to the following results for the Brazilian coast: increase in mean annual significant height (Hs) by ca. 6 mm/year; increase in Hs12 (Hs exceeded for 12 h on average every year, thus related to the annual extreme values; Hs is closely linked to the closure depth of the beach profile and thereby to potential erosion), with mean values of around 3 cm/year; a moderate (1.5 mm/year) increase in surge extremes was noted on the southern Brazilian coast, with a similar reduction in the northern coast; and a clockwise rotation trend in the direction of the mean energy flux (DFE; related to sediment transport and pocket beach rotation). The clockwise rotation trend is probably related to the previously detected trend of rotation toward the poles in extratropical storm activity, meaning more storm activity at high latitudes and less at medium latitudes, something which is more pronounced in the South Hemisphere (SH). The southern Atlantic coast shows low positive correlation according to the northward displacement of the Atlantic intertropical convergence zone. The correlation pattern, however, has strong similarities to the pattern of the Tropical South Atlantic Index (measures sea-surface temperatures in the eastern tropical South Atlantic Ocean), because both indices are related to Atlantic warming. In view of these results, no apparent link exists between El Niño–Southern Oscillation (ENSO/SOI) and wave climate on the South Atlantic coast, for either wave height or direction.

Despite the limited mapping scale, the data from wave climate reanalysis (1948–2008) presented by Reguero et al. (2013) and CEPAL (2016) allows us to identify some trends specifically for the coast of São Paulo State, such as mean annual Hs of 1.5 m; maximum mean Hs of 2.5 during June-July-August, and 3.8 m during September-October-Novenber; Hs12 ranging between 3.3 and 4.3 m; DFE of SSE (135–180°); astronomical tide ranges of 0.5–1.0 m; meteorological tide (storm surge influence) of 0.3–0.4 m on average. Considering only extreme events (Hs + storm surge) and return periods of 50 years (period of reanalysis) and 500 years (reference year: 2010), $Hs_{(50)}$ = 5.5–6.0 m; $Hs_{(500)}$ = 7.0–8.0 m; meteorological tide (50) = 1.3–1.8 m. The long-term (61-year time span) trends indicate the following increases in average values: Hs = 0.1–0.3 cm/year; Hs12 = 0.7–1.3 cm/year; DFE = 0.13–0.22°/year clockwise (values also increase northward along the state coast).

According to Losada et al. (2013) and CEPAL (2016), the annual trends in storm surge (SS) extremes indicated that the zone with the greatest positive trend was Río de la Plata, with values of up to 5 mm/year between 1948 and 2008. This was also the area with the greatest surge extremes throughout all seasons. Trends decreased to 2 mm/year immediately north of the river inlet, extending northward to Brazil's southern coast. The increase is associated with the 100-year return period level, which is at its greatest in northern Argentina, Uruguay and southern Brazil, where the trend is dominated by SS extremes (note that these areas are poles of cyclogenesis). At the remaining points, the mean sea level (MSL) trend predominates. Moreover, long-term shifts in extreme probability density functions suggest that extreme values have become more frequent in recent decades.

These results imply that coastal flooding risk in low-lying areas may be increasing due to a combination of rising MSL and variations in extreme SS events. By itself, rising MSL may not cause flooding, but rising water levels have caused a decrease in the return periods of the extreme total water levels during the last five decades (Losada et al. 2013).

Concerning climate extreme projections for the Brazilian coastal zone, trends point toward an increase in magnitude and frequency of extreme rainfall events (5 days), as well as a decrease in their return periods for all regions, the Southeastern and Southern Regions in particular, and an increase in wind velocity for all regions, the Northeast in particular (e.g. Magrin et al. 2014; CEPAL 2016; Marengo et al. 2017a). These trends, in addition to an increase in the SLR rate for the entire Brazilian coast, will likely increase the number and magnitude of natural disasters related to meteorological-oceanographic events, such as coastal erosion, coastal inundation and flooding.

This chapter presents an analysis of an extensive time series of hazardous events and associated processes, such as storm surges and coastal inundation/flooding, that have caused injuries and widespread human, material, economic or environmental losses in many areas of the Baixada Santista Metropolitan Region (BSMR).

6.2 Main Concepts

Storm surge (SS) is the abnormal rise in seawater level during a storm on an open coast, measured as the height of the water above the normal predicted astronomical tide, resulting from the combined impact of wind setup due to wind stress on the water surface, the atmospheric pressure reduction (cyclonic storm), decreasing water depth, and the horizontal boundaries of the adjacent water (Pugh 1987; NOAA 2017; Mangor et al. 2017). The "surge" is the difference between the observed and the predicted (astronomical tide) levels, which can be either positive or negative and causes a rapid increase or decrease in sea level (SL), respectively (Pugh 1987). Therefore, it corresponds to the meteorological tide. Storm tide is the total observed seawater level during a storm, resulting from the combination of storm surge and astronomical tide (NOAA 2017).

In summary, high winds and low pressure created by the cyclonic storm cause water to accumulate at this centre, resulting in water piling up along the front of the storm during its migration across the ocean (Pugh 1987). Closer to the shore, water is pushed toward the beach, causing a rapid elevation in SL, with waves becoming higher and more powerful. Consequently, an SS occurs. However, this complex phenomenon is further influenced by many different factors. The amplitude of the SS at any given location depends on the orientation of the coastline relative to the storm track; the intensity, size, and speed of the storm; and the local bathymetry and underwater topography (NOAA 2017; Mangor et al. 2017). The effects associated with atmospheric pressure are less than 10% of the total, wind shear stress on the sea surface being the main component (Camargo and Harari 1994; Marone and Camargo 1994).

In the southern region of South America, atmospheric circulation is controlled by atmospheric perturbation, particularly the South Atlantic Tropical Anticyclone—a wet and stationary (westerly winds) high pressure centre—and the cold migratory anticyclones, such as the Atlantic Polar Anticyclone, which are responsible for the northward migration of extratropical cyclones (southeastern winds) and associated cold fronts (e.g. Satyamurti et al. 1998).

South America has four cyclogenesis centres (Gan and Rao 1991; Sinclair 1996; Parise et al. 2009; Reboita et al. 2010) responsible for the formation and migration, or meteorological patterns, of extratropical cyclones: (a) Pattern I – cyclogenesis in the southern Argentinian coast, with a displacement to the east and a trajectory between 47.5°S and 57.5°S; (b) Pattern II – cyclogenesis in the southern Uruguayan coast, with a displacement to the east and a trajectory between 28°S and 43°S; (c) Pattern III – cyclogenesis in the southern Uruguayan coast, with a displacement to the southeast and a trajectory between 32°S and 57.5°S; (d) Pattern IV – high-pressure centre generating easterly winds.

Machado et al. (2010) conducted a hindcast study of wave energy in deep water (100 m), using a wave model based on reanalysis of 29 years (1979–2008) of wind data for the coast of Rio Grande do Sul. They identified a total of 40 extreme events, 53.66% of which had a Pattern II trajectory, while 26.82% were associated with

Pattern III; collectively, these patterns represented 80% of all extreme events. Coastal erosion episodes were associated mostly with Pattern II, while Pattern III caused the highest surges.

Parise et al. (2009) studied extreme SS in southern Brazil and concluded that the highest sea level elevation events resulted from the action of SW winds, which blow parallel to the main NE-SW coastline orientation in the region, and may be explained by the Coriolis effect (i.e. Ekman transport) causing a build-up of water along the coast.

Another way to retrieve and analyse historical data on extreme meteorological-oceanographic events is through a survey of articles from local and regional news media. Paula et al. (2015) called this type of survey the "hemerographic method". Examples of this approach being used in Brazil can be found in the works of Bittencourt et al. (2008), Lins-de-Barros (2010), Pontes and Zee (2010), Paula et al. (2015), and Rudorff et al. (2014).

Chapter 8 also surveys news articles, as sources of information on the occurrence of mass movements.

6.3 Coastal Processes and Extreme Events in Santos

In general, on any ocean coastline, SS has the following results:

(a) Beach erosion – due to the transfer of sediments from the immersed/subaerial contour to the submerged contour of the beach (Bruun rule), and the temporary transverse/vertical migration of the beach contour in the direction of the mainland;
(b) Erosion of urban infrastructure and retention structures – due to the hydraulic and mechanical forces generated by the waves (overtopping) on these structures;
(c) Coastal inundation – due to the raised elevation of the SL and the overtopping of waves over urban structures.

Coastal erosion (of the entire coastline) can be classified as chronic or acute (e.g. Mangor et al. 2017). Normally, coastal erosion develops progressively and continuously over the years. This happens due to the deficit in the sedimentary balance of a given coastal cell. Acute erosion results from extreme events, such as storm surges (waves heights greater than normal) and positive meteorological tides (short-term sea level rise), whose effect is the migration of the beach profile toward the mainland and the displacement of large quantities of sand to the immersed contour of the beach (e.g. Souza 2009a, b, 2012).

The consequences of coastal erosion can be diverse – a reduction in the width of the beach and/or retrogradation of the coastline; disappearance of the backshore and even of the beach itself; loss of properties and assets along the coastline; destruction of man-made structures parallel and transverse to the coastline; problems with, or collapse of, the sanitation drainage system (underground systems and marine

outfall); reduction of the recreational water quality of coastal waters; erosion in the region downstream of estuarine ecosystems, with possible alteration of estuarine circulation; loss of fishery resources; loss of scenic value of the beach and/or coastal region; loss of the property value of oceanfront homes; compromised tourism potential of the region; impairment of socioeconomic activities connected to beach-related tourism and leisure; artificial construction of the coastline (coast "protection" structures); increased expenses due to restoration of beaches and reconstruction of the waterfront (Souza et al. 2005; Souza 2009a, 2012).

In Santos, chronic erosion has affected Ponta da Praia since the beginning of the 1940s, triggered mainly by the construction of the avenue to the waterfront over the beach itself (Souza et al. 2012; Souza 2017). Further contributions to this erosion include destruction of the dunes, coastal strands and mangroves; alterations to the drainage network; increasing impermeability of the land close to the coastline; landfills above the estuarine channel; installation of structures transverse to the coastline; construction of retaining walls and stone bulkheads; dredging (mainland and Santos Bay); removal of sand from the beach; sea-level rise; and increased occurrence of extreme events (storm surges and meteorological tides).

On the short- and mid-term temporal scale, the morphodynamic processes of Praia de Santos are controlled by the occurrence of extreme meteorological-oceanographic events (Souza et al. 2016a, b; Souza 2017). In the east-southeast sector (Southeast Zone) of the beach (Fig. 6.1), these events cause acute erosion of the beach and destruction of urban infrastructure, and they intensify the chronic erosion of Ponta da Praia and its expansion toward Canal 4, as well as provoking coastal flooding in the Ponta da Praia region and, eventually, the waterfront of neighbourhoods adjacent to Canal 4 (Fig. 6.2).

Costal inundation has also affected the Northwest Zone of Santos (see Fig. 6.1). This area also suffers with flooding caused by intense rains and high concentration of surface runoff, influenced by the drainage network coming from the hills of Santos; the low declivity of the entire region; the increasing impermeability of the land (this region was largely built over old mangroves and wetlands); the inefficiency of the urban macro-drainage system; and the damming of water in the mouth of the basin (man-made channel) connected to the estuary, which is provoked by high tides, especially during spring tides. What occurs in the area is a sum of processes that trigger coastal inundation and flooding.

In addition to the costs of the restoration of Ponta da Praia and the continual maintenance of the sanitation canals, the greatest socioeconomic harm arising from these extreme events in Santos is related to loss and damage of the public and private natural heritage, due to coastal erosion; coastal inundation; flooding in lowlands; siltation in the navigation channel; damage to coastal protection works; structural or operational damage to Santos Port and terminals; damage to urban structures; flooding of the underground parking of buildings; structural damage or operational damage to sanitation and port infrastructure works; exposure of buried pipelines or structural damage to exposed pipelines; and serious disruption of the functioning of coastal communities, especially transportation and services.

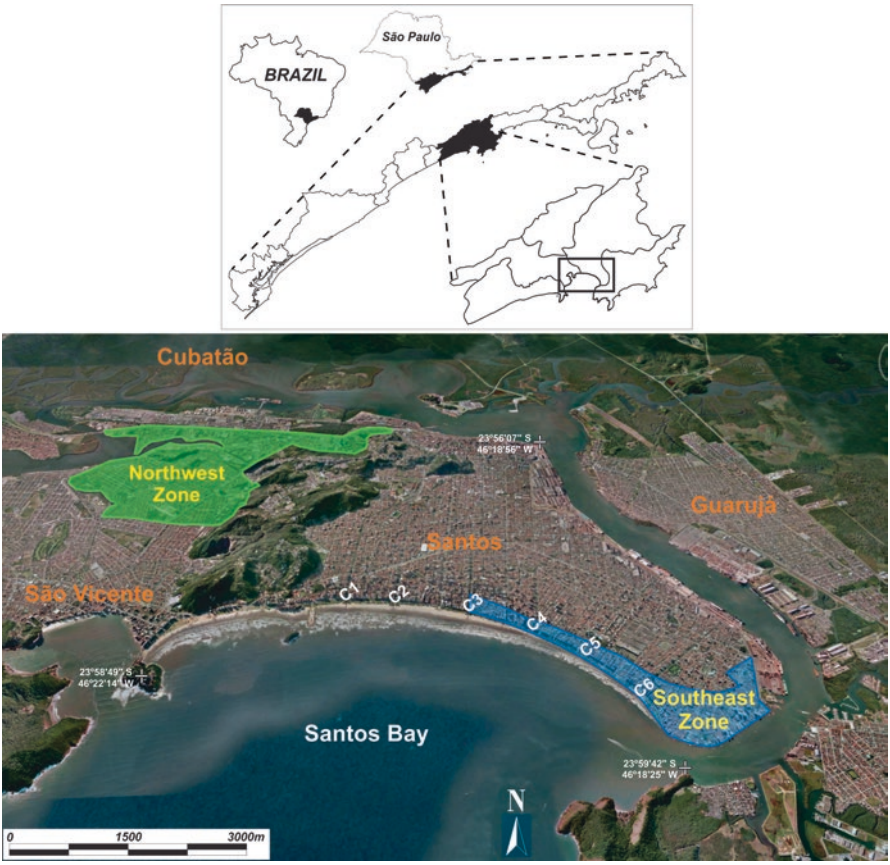

Fig. 6.1 Areas in Santos most affected by storm surges, causing coastal erosion and coastal inundation/flooding (C1–C6 = man-made drainage canals)

6.4 Data Bank Framework and Indicators of Boundary Conditions

The database presented here includes a historical analysis, using the hemerographic method, of the occurrence of extreme meteorological-oceanographic events that affected the region. These events are reported in the media as "*Ressacas*" (storm surges) and "*Marés Altas*" (high tides). In fact, they correspond to one type of hazard (storm surge) and its associated geodynamic processes, including coastal erosion, coastal inundation and flooding. In this case, flooding is caused by the combination of heavy rainfall and high tides, so that the waters from the watersheds discharges summed to the superficial continental runoff flowing down are blocked by the tidal waters rising into the existing drainage system (Marengo et al. 2017b).

Fig. 6.2 Some impacts caused by storm surges on 07/04/2015 (**a**), 06/08/2016 (**b**), 16-08/2017 (**c**) and 20/05/2018 (**d**) in Ponta da Praia region (Southeast Zone) (photos from the first author)

The research focused mainly on the largest regional newspaper, *A Tribuna de Santos*, through both its physical (since 1928) and online (www.atribuna.com.br/) archives. Other newspapers, such as *Diário do Litoral, Expresso Popular, Jornal da Tarde, D.O. Urgente*, served as complementary references. News and information on oldest historical events were also consulted on the website *Novo Milênio* (www.novomilenio.inf.br/).

Generally, these events are only reported on by the newspapers when they significantly alter the beaches and/or cause some disruption for the city. In other words, most of the reports refer to events of high intensity and magnitude; therefore, we refer to them here as "extreme events".

It must be noted that most of the news reports refer to Santos, home of the surveyed newspapers. As the urbanisation in Santos seaside dates back to the beginning of 1930s, we can assume that an absence of news is not due to a lack of urbanisation.

For comparison, we also consulted the extreme events registry – *Cadastro de Eventos Extremos* – developed by the Geological Institute for the period 1923–2010 (Gutjahr 2011), and the climate studies registry – *Cadastro do Laboratório de Estudos Climáticos* – of the Institute of Geosciences/Unicamp (LECLIG, for *Laboratório de Estudos Climáticos do Instituto de Geociências* in Portuguese), covering the period 1928–2014.

6.4.1 Methodological Approach

The meteorological-oceanographic events are influenced by a set of forcings linked to winds, waves, tides, lunar phase, precipitation, atmospheric circulation at the regional scale, and climate phenomena at the global scale, such as the El Niño Southern Oscillation (ENSO).

Regarding the atmospheric phenomena that influence these events in the state of São Paulo, the studies of Campos et al. (2010) were pioneering. The authors analysed a historical series (1951–1990) of data for wind fields, surface pressure, and sea level rise to identify SS in the Baixada Santista region and to compare them to some high-intensity occurrences that caused significant damages to Santos. The results showed that SS occurred due to the migration and persistence of a low-pressure system (extratropical cyclone) over the ocean, moving from southern South America, as well as the action of an anticyclone over the continent for a period of days, with winds above 8 m/s acting upon the ocean near the coast. The authors concluded that, in general, 2 days before an event of maximum sea level elevation is felt in Santos, an associated cold front is positioned over the coast of Paraná and São Paulo; one day before, the front passes over Santos, moving to Rio de Janeiro; and on the day of peak SS in Santos, the cold front reaches Espirito Santo. The period of greatest SS activity occurs between autumn and winter (April and August) and appears to depend on the intensification, size and position of the troughs over the ocean. In both the autumn and the winter, there are intense SW winds approximately parallel to the coast, a pattern determined by the troughs over the ocean in conjunction with high pressure over the mainland, increasing the number of SS events. In winter, severe intensification of the anticyclone over the mainland increases the pressure gradients responsible for intense SW winds; this period has the highest incidence of extreme cases. Conversely, in spring and summer, the troughs weaken, and the wind intensity diminishes, reducing the occurrence of events. For the analysed series, the distribution of events was as follows: 14.5% in spring; 13.4% in summer; 40.2% in autumn; and 30.8% in winter. Comparing the considered decades, the authors observed an increasing trend in the number of positive extremes between 1951 and 1980, of the order of 13%.

Thus, to determine the boundary conditions of each event registered by the data banking we selected seven indicator groups:

(a) Duration and evolution intervals of the events
(b) Lunar phase
(c) Maximum height of the meteorological tide
(d) Precipitation accumulated in the duration and evolution intervals of the event
(e) Direction and intensity of the winds in the region
(f) Significant wave height and direction in the region
(g) Correlation with phases of El Niño and La Niña

6.4.1.1 Duration and Evolution of Events

The "duration interval" of the event was defined as being the period between the actual start date of the event (not necessarily of the news about it) and last news report on the same event.

Considering the results of Campos et al. (2010), we defined the "evolution period" of the event, which encompasses 4 days prior to the beginning of the event in addition to the "duration interval". This period was used for synoptic analysis of the events and to obtain rainfall accumulations.

6.4.1.2 Lunar Phase

Record of the lunar phase for each event was obtained from websites (http://www.cosmobrain.com.br and http://magodosol.atspace.org/lua).

The phases of greatest sea level rise occurred during the full and new moons, i.e. during spring tides, while the least SLR occurred during neap tides. Some events can occur in transition phases or extend over more than one lunar phase. Thus, to represent the different phases, we adopted the scale shown in Table 6.1.

6.4.1.3 Meteorological Tide

The tidal regime on the coast of São Paulo is semi-diurnal with diurnal inequality, having two high tides and two low tides at approximately 6-h intervals, the nocturnal high tide generally being the highest.

To describe this indicator, the highest meteorological tide levels were used for the duration interval; these values were made available by the Institute of Oceanography of the University of São Paulo (historical series of the Torre Grande tide gauge and satellite altimetry data) and the Hydrodynamic Research Centre at the University of Santa Cecília (measuring instrument of the Praticagem as of 2015).

It must be stressed that, because the data is from different sources, the results should be interpreted with caution.

Table 6.1 Values attributed to lunar phases for showing in graphic representation

Lunar Phase	Value
Full/waning	0.5
Waning	1
Waning/new	1.5
New	2
New/waxing	2.5
Waxing	3
Waxing/full	3.5
Full	4

6.4.1.4 Rainfall Volume

Rainfall data were acquired from the pluviometric databases of Santos provided by the Caete station (DAEE E3-041, 23°53′00″S/46°13′00″W, 200-m high) and the Saboó station (DNAEE-02316279, originally located at 23°56′06″S/46°20′22″W, 60-m; currently at 23°55′12″S/46°20′40″W, 32-m), and from the rainfall index of the Santos Municipal Government (www.santos.sp.gov.br/indicepluviometrico). The Caete station covers the period 1937–2004, and the Saboó station, from 1939 onward.

The data from the Saboó station were also analysed in Chaps. 3 and 8.

Between the data from the two stations, we always selected the highest volume and accumulated totals for the duration interval and evolution period (duration interval + 4 days prior to the beginning of the event).

For the data analysis, the cumulative rainfall data were divided into range classes (Table 6.2), chosen according to previous studies on accumulated minimum rainfall for flooding/inundation development in other coastal regions of the state of São Paulo (Santana et al. 2004; Souza 2009c).

6.4.1.5 Waves, Winds and Synoptic Charts

The wind and wave data were compiled from databases provided by the following institutions: National Bank of Oceanographic Data of the Brazilian Navy (BNDO/DHN, for *Banco Nacional de Dados Oceanográficos – Diretoria de Hidrografia e Navegação*), National Institute for Space Research (INPE-CPTEC, for *Instituto Nacional de Pesquisas Espaciais – Centro de Previsão de Tempo e Estudos Climáticos*) and Hydrodynamic Research Centre of the University of Santa Cecília (Unisanta).

The data from BNDO/DHN (the *Meteoromarinha* bulletins) include the oldest historical series, starting in 1941, though it contains many gaps. Until November 1978, these bulletins presented descriptive (not numerical) information about the intensity of the winds, significant wave heights and general direction of wind and waves. We therefore transformed the information on wind intensity and wave height into numerical data based on the Beaufort and Sea State scales (available on the website of the DHN), respectively. The absence of wave period data until November

Table 6.2 Rainfall accumulation classes for duration interval and evolution period

Time	Duration interval	Evolution period
Rainfall (mm)	0–60	0–100
	61–120	101–200
	121–180	201–300
	181–240	>300
	>240	

1978 was the reason that this attribute was not used as a descriptor of the events' boundary conditions.

The data provided by the INPE-CPTEC derived from simulations made by the model WAVEWATCH, implemented in Brazil in March 2006. For the Baixada Santista, the model has a spatial resolution of 1 × 1°, over an area centroid of 24°S and 46°W.

The data provided by Unisanta is also on a regional scale and is based on SWAN wave models and NOAA meteorological models, with wave data starting in October 2014 and wind data since December 2015 (Ribeiro et al. 2016).

The values entered into the present database (for the event duration interval) were always the highest among all available data sources. For the wind and wave direction data, the azimuth notations were transformed into numerical values (0–360°), and then the average of the values was used.

It must be noted that, due to different data sources and types of collection/modelling, the presented results should be interpreted with caution.

The synoptic charts (BNDO and INPE-CPTEC) were used to analyse the synoptic evolution of the atmospheric systems and validate the news reports.

6.4.1.6 El Niño and La Niña

To characterise the active phases of ENSO – El Niño and La Niña – we consulted the INPE-CPTEC website for the historical series 1877–2010 (http://enos.cptec.inpe.br/) and the NOAA website for the period 1950–2017, based on the Oceanic Niño Index – ONI (http://www.cpc.ncep.noaa.gov/products/analysis_monitoring/ensostuff/ensoyears2011.shtml), as well as another compilation organised into annual intervals and based on the ONI (http://ggweather.com/enso/oni.htm).

The available data indicates the active year and the classification of the phenomenon, such as very strong to strong, medium and weak intensities (Table 6.3), which is based on the pattern and magnitude of anomalies of the Tropical Pacific Sea Surface Temperature.

Table 6.3 ENSO phases and attributed intensity values

Intensity	El Niño	La Niña
Very strong-strong	3	−3
Moderate	2	−2
Weak	1	−1
Neutrality	0	0

6.5 Storm Surges and Coastal Inundation/Flooding Events: Boundary Conditions

Table 6.4 presents a list of events registered between 25 April 1928 and 28 October 2016, as well as some earlier ones, in which *Storm Surge* and *Coastal Inundation/Flooding* are referred to as SS and CI/F, respectively.

The first storm surge and high tide event registered in the region, and in Brazil, occurred in 1541, called the "tsunami" of de São Vicente in historical documents. The consequences were determinants of the region's history, with the near total destruction of then Vila de São Vicente, and the relocation of the port there to the opposite end of Ilha de São Vicente, where the Povoado do Porto de Santos and, later, the Vila de Santos were built. In 1580, another strong event occurred, destroying part of the then reconstructed Vila de São Vicente. There are records of strong storm surges in the years 1905, 1908, 1914, 1927 and 1946; however, the exact dates are unknown.

Most of the events compiled refer to the municipality of Santos, but may also involve other municipalities or all of the Baixada Santista, and may even include all of coastal São Paulo. News articles that do not cite Santos account for 37 events (13 SS and 24 CI/F), which correspond to 15.6% of the total. These events refer mainly to São Vicente, a contiguous neighbour located on the same island.

Some of the indicators that depend on measurements in the field, such as winds, waves, rain and real tides, present several gaps in their data series, especially prior to the mid-twentieth century. Hence, for these indicators, the statistical analyses do not represent the totality of registered events.

6.5.1 General Characteristics

Between 1928 and 2016, 238 extreme events were registered (see Table 6.4), among them 115 SS (48%) and 123 CI/F (52%). Fifty of these events, or 21%, were simultaneously SS and CI/F.

In the graphic showing the annual distribution of these events (Fig. 6.3), a large increase is evident in the number of extreme events per year, especially SS, starting in 1999. Between the 1920s and 1970s, there were 19 CI/F events and 9 SS events. In the 1980s, the number of events increased considerable, with 33 CI/F and 12 SS. In the 1990s, the number decreased, totalling 13 CI/F and 6 SS, 4 of which occurred in 1999 alone. In the 2000s, the number of SS jumped to 49, and CI/F events increased to 24. The year 2010 had the highest number of events, with 14 SS and 3 CI/F, followed by 2009 (11 SS and 5 CI/F) and 2016 (10 SS and 6 CI/F).

Also evident is an increase, starting in the 1980s, of the number of consecutive years in which both types of events occurred, eventually becoming yearly. The only years without any record of extreme events during the studied period were 1993,

Table 6.4 Historical series of Storm Surges (SS) and Coastal Inundation/Flooding (CI/F) records

ID	Type	Date	Affected area	ID	Type	Date	Affected area	ID	Type	Date	Affected area
	SS/CI/F	1541	São Vicente Village	**78**	CI/F	04/08/1992	São Vicente	**159**	CI/F	16/09/2008	Santos
	SS/CI/F	1580	Santos, São Vicente	**79**	CI/F	12/01/1994	São Vicente	**160**	SS	03/01/2009	Santos
	CI/F	1905, 1908	Santos	**80**	CI/F	28/01/1994	Baixada Santista	**161**	SS	25/02/2009	Baixada Santista
	SS	1914, 1927,194«	Santos/São Vicente	**81**	CI/F	06/02/1994	Baixada Santista	**162**	CI/F	25/02/2009	Baixada Santista
1	CI/F	25/04/1928	Santos	**82**	CI/F	09/03/1995	São Vicente	**163**	SS	11/04/2009	Santos/São Vicente
2	CI/F	10/01/1948	São Vicente	**83**	SS	12/02/1996	São Paulo Littoral	**164**	CI/F	11/04/2009	Santos/São Vicente
3	CI/F	01/03/1956	Santos	**84**	CI/F	12/02/1996	São Paulo Littoral	**165**	SS	16/04/2009	Santos
4	CI/F	27/03/1956	Santos	**85**	CI/F	04/03/1996	Santos/São Vicente	**166**	SS	03/06/2009	Santos
5	CI/F	30/09/1961	Santos	**86**	CI/F	20/03/1996	Baixada Santista	**167**	SS	20/07/2009	São Vicente
6	SS	30/09/1961	Santos	**87**	SS	07/04/1997	Santos/São Vicente	**168**	SS	24/07/2009	São Vicente
7	CI/F	08/03/1966	Santos	**88**	CI/F	07/04/1997	Santos/São Vicente	**169**	SS	30/07/2009	São Vicente
8	CI/F	20/11/1969	Santos	**89**	SS	18/04/1999	São Vicente	**170**	CI/F	30/07/2009	São Vicente
9	CI/F	16/12/1970	Santos	**90**	SS	21/05/1999	Santos	**171**	SS	21/08/2009	São Vicente
10	SS	01/01/1971	Baixada Santista	**91**	SS	31/05/1999	Baixada Santista	**172**	SS	08/09/2009	Santos
11	CI/F	01/01/1971	Baixada Santista	**92**	SS	15/08/1999	Guarujá	**173**	CI/F	08/09/2009	Santos
12	CI/F	16/02/1971	Baixada Santista	**93**	SS	16/07/2000	Santos	**174**	SS	24/09/2009	Santos
13	SS	26/02/1971	Santos	**94**	CI/F	16/07/2000	Santos	**175**	CI/F	02/12/2009	São Vicente
14	CI/F	26/02/1971	Santos	**95**	CI/F	12/01/2001	Santos	**176**	SS	26/02/2010	Santos/São Vicente
15	CI/F	16/01/1973	Baixada Santista	**96**	SS	05/05/2001	São Vicente	**177**	CI/F	26/02/2010	Santos/São Vicente
16	CI/F	23/02/1975	Baixada Santista	**97**	CI/F	05/05/2001	São Vicente	**178**	SS	17/03/2010	São Vicente
17	CI/F	28/02/1975	Santos	**98**	SS	21/06/2001	Santos/Guarujá	**179**	CI/F	17/03/2010	São Vicente
18	CI/F	28/01/1976	Santos	**99**	SS	27/07/2001	Santos	**180**	SS	08/04/2010	Santos/São Vicente
19	CI/F	25/03/1976	Santos	**100**	SS	17/09/2001	São Paulo Littoral	**181**	SS	09/05/2010	Santos
20	CI/F	24/12/1976	Baixada Santista	**101**	CI/F	17/09/2001	São Paulo Littoral	**182**	SS	13/07/2010	Santos
21	CI/F	02/04/1977	São Vicente	**102**	SS	16/01/2002	Santos	**183**	SS	27/07/2010	Santos

ID	Type	Date	Affected area	ID	Type	Date	Affected area	ID	Type	Date	Affected area
22	SS	17/05/1977	Baixada Santista	**103**	CI/F	16/01/2002	Santos	**184**	SS	02/08/2010	Baixada Santista
23	SS	09/03/1978	Santos	**104**	SS	21/03/2002	Santos/São Vicente	**185**	SS	11/08/2010	Santos
24	CI/F	09/03/1978	Santos	**105**	CI/F	29/03/2002	Santos	**186**	SS	05/09/2010	Santos
25	SS	31/05/1978	Santos	**106**	SS	22/05/2002	Santos/São Vicente	**187**	SS	18/09/2010	Santos
26	SS	18/07/1978	Santos	**107**	SS	17/06/2002	Santos	**188**	SS	08/10/2010	Baixada Santista
27	SS	22/07/1979	Santos	**108**	SS	10/07/2002	São Vicente	**189**	CI/F	08/10/2010	Baixada Santista
28	SS	02/01/1980	Baixada Santista	**109**	SS	02/09/2002	Santos	**190**	SS	18/10/2010	Santos
29	CI/F	02/01/1980	Baixada Santista	**110**	SS	07/11/2002	Santos/São Vicente	**191**	SS	11/11/2010	Santos
30	CI/F	15/03/1980	São Vicente	**111**	CI/F	21/01/2003	Santos	**192**	SS	13/12/2010	Santos, Guarujá
31	CI/F	01/08/1980	São Vicente	**112**	CI/F	18/02/2003	Santos	**193**	SS	14/03/2011	Santos
32	SS	17/08/1980	Santos	**113**	SS	21/03/2003	Santos	**194**	CI/F	14/03/2011	Santos
33	CI/F	22/12/1980	Santos	**114**	CI/F	21/03/2003	Santos	**195**	SS	03/05/2011	Baixada Santista
34	CI/F	22/01/1981	Santos	**115**	SS	12/04/2003	Santos	**196**	CI/F	03/05/2011	Baixada Santista
35	CI/F	17/03/1981	São Vicente/Cubatão	**116**	CI/F	12/04/2003	Santos	**197**	SS	28/05/2011	Santos/São Vicente
36	SS	08/06/1981	São Vicente	**117**	SS	25/05/2003	Santos	**198**	SS	08/06/2011	Santos
37	CI/F	08/06/1981	São Vicente	**118**	CI/F	25/05/2003	Santos	**199**	SS	20/08/2011	Santos
38	CI/F	16/10/1981	Santos/São Vicente	**119**	SS	12/07/2003	Santos/São Vicente	**200**	CI/F	19/07/2013	Santos
39	CI/F	14/07/1982	São Vicente	**120**	CI/F	09/01/2004	Santos/Guarujá	**201**	CI/F	17/01/2014	Santos
40	SS	19/09/1982	Santos/São Vicente	**121**	SS	29/02/2004	Baixada Santista	**202**	CI/F	03/03/2014	Santos
41	CI/F	19/09/1982	Santos/São Vicente	**122**	CI/F	06/03/2004	Santos	**203**	SS	14/04/2014	Santos
42	SS	28/09/1982	São Vicente	**123**	SS	07/05/2004	Baixada Santista	**204**	CI/F	14/04/2014	Santos
43	CI/F	28/09/1982	São Vicente	**124**	SS	12/05/2004	Santos	**205**	CI/F	26/04/2014	Santos
44	SS	14/10/1982	São Vicente	**125**	SS	21/05/2004	Santos	**206**	CI/F	06/05/2014	Santos
45	CI/F	14/10/1982	São Vicente	**126**	SS	28/05/2004	Santos	**207**	CI/F	25/07/2014	Santos
46	CI/F	02/02/1983	Santos	**127**	CI/F	28/05/2004	Santos	**208**	SS	28/08/2014	Santos

(continued)

Table 6.4 (continued)

ID	Type	Date	Affected area	ID	Type	Date	Affected area	ID	Type	Date	Affected area
47	CI/F	03/06/1983	Santos/São Vicente	**128**	SS	12/06/2004	Santos/São Vicente	**209**	CI/F	28/08/2014	Santos
48	CI/F	11/06/1983	Baixada Santista	**129**	SS	22/03/2005	Santos	**210**	CI/F	22/12/2014	Santos/São Vicente
49	CI/F	12/07/1983	Santos	**130**	SS	26/04/2005	Santos	**211**	CI/F	24/01/2015	Santos
50	CI/F	25/10/1983	São Vicente	**131**	SS	21/05/2005	Santos/São Vicente	**212**	CI/F	30/01/2015	Santos
51	SS	28/06/1984	Santos	**132**	SS	06/07/2005	Santos	**213**	SS	06/04/2015	Santos
52	CI/F	28/06/1984	Santos	**133**	SS	11/02/2006	Santos	**214**	CI/F	06/04/2015	Santos
53	CI/F	06/04/1985	Santos	**134**	CI/F	27/03/2006	Santos	**215**	SS	20/04/2015	Santos
54	SS	07/06/1985	Santos/São Vicente	**135**	CI/F	17/05/2006	Santos	**216**	SS	19/06/2015	Santos
55	CI/F	07/06/1985	Santos/São Vicente	**136**	SS	28/06/2006	Santos	**217**	SS	25/06/2015	Santos
56	CI/F	26/03/1986	Santos	**137**	CI/F	28/06/2006	Santos	**218**	SS	23/07/2015	Santos
57	SS	15/04/1986	Santos	**138**	SS	30/07/2006	Guarujá	**219**	SS	02/09/2015	Santos
58	CI/F	15/04/1986	Santos	**139**	CI/F	30/07/2006	Guarujá	**220**	CI/F	19/09/2015	Santos
59	SS	21/07/1986	Santos	**140**	SS	21/08/2006	Guarujá	**221**	SS	17/10/2015	Santos
60	CI/F	21/07/1986	Santos	**141**	SS	04/09/2006	Santos/Guarujá	**222**	SS	07/11/2015	Santos
61	CI/F	02/12/1986	Cubatão	**142**	CI/F	04/09/2006	Santos/Guarujá	**223**	SS	21/04/2016	Santos
62	CI/F	17/03/1987	Santos	**143**	CI/F	05/10/2006	Baixada Santista	**224**	SS	27/04/2016	São Paulo Littoral
63	CI/F	23/01/1988	Baixada Santista	**144**	CI/F	16/10/2006	Santos	**225**	CI/F	27/04/2016	São Paulo Littoral
64	CI/F	06/02/1988	Baixada Santista	**145**	SS	09/11/2006	Santos	**226**	SS	16/05/2016	Santos
65	CI/F	21/02/1988	São Paulo Littoral	**146**	CI/F	09/11/2006	Santos	**227**	SS	11/06/2016	Santos
66	CI/F	03/04/1988	Santos	**147**	SS	27/04/2007	Guarujá	**228**	SS	18/07/2016	Santos
67	CI/F	02/06/1988	São Vicente	**148**	SS	25/05/2007	Santos	**229**	CI/F	18/07/2016	Santos
68	CI/F	30/06/1988	São Vicente	**149**	SS	28/05/2007	Santos	**230**	SS	28/07/2016	Santos
69	SS	10/08/1988	Guarujá/São Vicente	**150**	CI/F	28/05/2007	Santos	**231**	SS	11/08/2016	Santos
70	CI/F	10/08/1988	Guarujá/São Vicente	**151**	SS	28/07/2007	Santos	**232**	CI/F	11/08/2016	Santos
71	CI/F	20/04/1989	Santos	**152**	CI/F	28/07/2007	Santos	**233**	SS	21/08/2016	São Paulo Littoral

72	SS	17/09/1989	Santos/São Vicente	**153**	CI/F	16/10/2007	Santos	**234**	CI/F	21/08/2016	São Paulo Littoral
73	SS	23/05/1990	Santos	**154**	SS	17/11/2007	Santos	**235**	SS	15/09/2016	São Paulo Littoral
74	CI/F	23/05/1990	Santos	**155**	CI/F	26/02/2008	Santos	**236**	CI/F	15/09/2016	São Paulo Littoral
75	CI/F	22/06/1990	São Vicente	**156**	SS	16/06/2008	Santos/São Vicente	**237**	SS	28/10/2016	São Paulo Littoral
76	CI/F	20/07/1990	São Vicente	**157**	CI/F	16/06/2008	Santos/São Vicente	**238**	CI/F	28/10/2016	São Paulo Littoral
77	CI/F	07/10/1991	Baixada Santista	**158**	CI/F	26/07/2008	Santos/São Vicente				

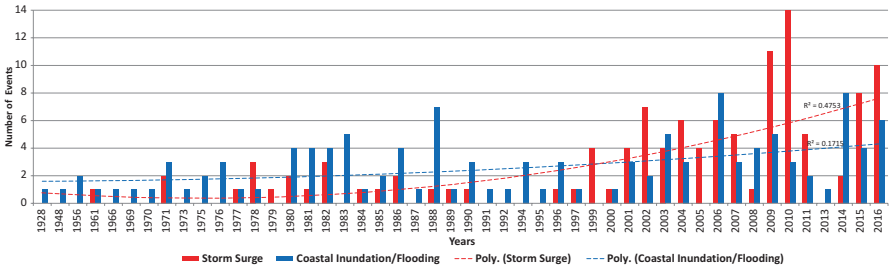

Fig. 6.3 Annual distribution of storm surges and coastal inundation/flooding events

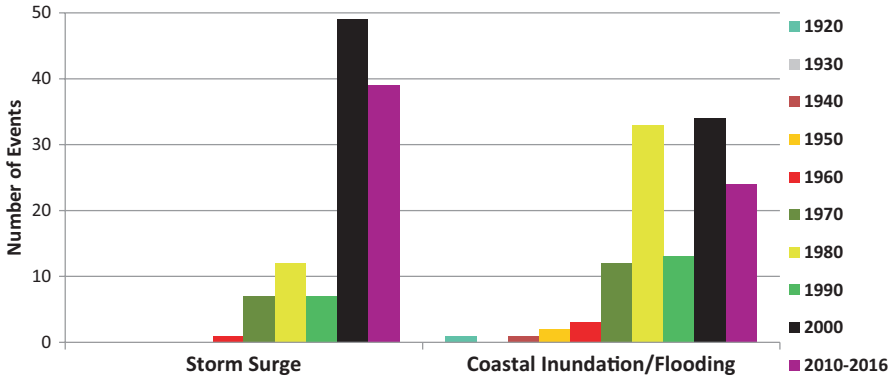

Fig. 6.4 Decadal distribution of storm surges and coastal inundation/flooding events

1998 and 2012. The 1970s seem to have been a transition, with SS becoming ever more frequent and in greater numbers per year.

The distribution of events per decade (Fig. 6.4) shows that the largest number occurred in the 2000s, which had 83 occurrences (35% of the 238 events), comprising 49 SS (42.6% of the 115 registered events) and 34 CI/F (27.6% of the 123 registered). The 2010s also look promising, since 65 events had already occurred in only half of the decade (39 SS and 24 CI/F). Therefore, in the last 17 years alone (2000–2016), there have been 146 events (61.3% of the total), of which, 88 (76.5%) are SS and 58 (47.2%) are CI/F. The 1930s was the only decade without registered events. SS has appeared only from the 1960s onward.

Another interesting fact is the occurrence of combined events, whose number increased to 10 in the 1980s, compared to 1 in the 1960s and 3 in the 1970s (and none before 1960). In the 1990s, the number of occurrences decreased again, occurring only three times. However, the number jumped to 19 in the 2000s, and there were 14 between 2010 and 2016. As these combined events are of greater magnitude, affecting all of Baixada Santista and, generally, other sectors of coastal São Paulo, we may conclude that the number of very strong events increased starting in the 2000s.

Table 6.5 Distribution of events along the centuries and rates of increase

Century (years)	SS (no)	Cl/F (no)	ALL (no)	% SS (115)	% Cl/F (123)	Rate SS (no/year)	Rate Cl/F (no/year)	Rate ALL (no/year)
XX (1928–1999)	27	65	92	23.5	52.8	0.4	0.9	1.3
XXI (2000–2016)	88	58	146	76.5	47.2	5.2	3.4	8.6
Rate of Increase	3.3	0.9	1.6	226.0	10.8	13.6	3.8	6.7

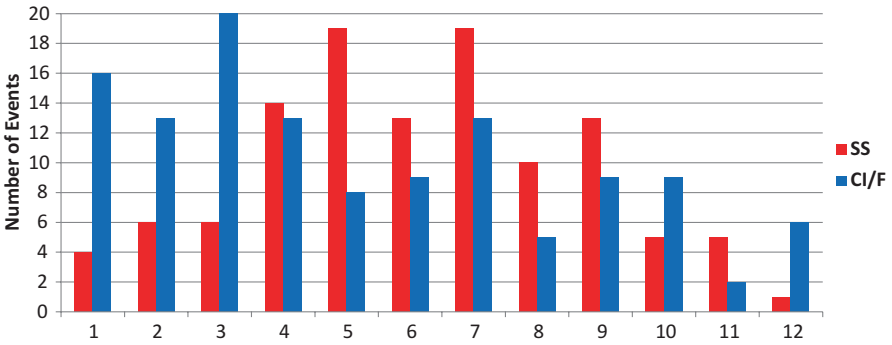

Fig. 6.5 Monthly distribution of occurrence of storm surges (SS) and coastal inundation/flooding (CI/F) events

Analysis of SS event distribution per century (Table 6.5) shows that the twentieth century, specifically 1928–1999 (72 years), had 27 events (23.5% of the total), which represents an average of 0.4 event/year. In the twenty-first century, in only the first 17 years (2000–2016), there have been 88 events (76.5% of the total), which corresponds to an average rate of 5.2 events/year. This indicated an increase in the number of events by 3.3 times (226%) in the twenty-first century, or an increase in the rate of events/year by 13.6 times, relative to the twentieth century. For CI/F, 65 events happened in the twentieth century (52.8%), indicating a rate of 0.9 event/year; while in the twenty-first century, 58 events have occurred (47.2%) at a rate of 3.4 events/year. Therefore, the increase in CI/F this century is 0.9 times the number of events and 3.8 times the rate of events/year.

In terms of the monthly distribution of events (Fig. 6.5), although both types occurred in all months, some key trends are highlighted above.

July was the month with the most events, totalling 32 (19 SS and 13 CI/F), followed by April (14 SS and 13 CI/F) and May (19 SS and 8 CI/F), both with 27 events each, while March had 26 (6 SS and 20 CI/F). The months with the fewest occurrences were November (5 SS and 2 CI/F) and December (1 SS and 6 CI/F), with seven events each.

The distribution of SS is most concentrated between April and September (cyclone/SS season, autumn/winter), totalling 76.5% (88 occurrences); May and

July had the highest number (19 each). These results are similar to those obtained by Campos et al. (2010), which showed that 71% of SS events occurred in autumn/winter (in a time series for 1951–1990).

CI/F occurs mainly between January and April, making up 50.4% of these events, with most happening in March (20), followed by January (16). The summer months alone (January–March) had 39.8% of events (49), while the autumn/winter had 46.3% (57). These results show that the CI/F are controlled by the more intense rains during the summer, often triggering flooding, and then by the effects of the cyclone/SS season and the steric effect (warming of the ocean during the summer) in autumn/winter, when the main process is coastal inundation. This assertion is supported by reports of combined events (those of greater magnitude), since among those 50 events, 11 occurred in the summer months, and 39 in the autumn/winter months.

December and January had the fewest SS events, and November and August had the fewest CI/F.

6.5.2 Duration of Events

The time span of each event's duration interval varied from 1 to 8 days (Fig. 6.6). For SS, the average duration interval was 1.9 days (variation of 1–8 days, with standard deviation of 1.4) and for CI/F, 1.8 days (variation of 1–5 days, with standard deviation of 1.1).

Around 49.2% of all events had a 1-day duration (4.6% of SS and 52% of CI/F). Events of 2- or 3-day duration totalled 40.3%; 9.2% lasted 4 or 5 days, and only 1.3% of SS events lasted for 7–8 days.

In the 2000s and 2010s, the SS events were of notably longer duration, particularly in the years 2007, 2010, 2015 and 2016.

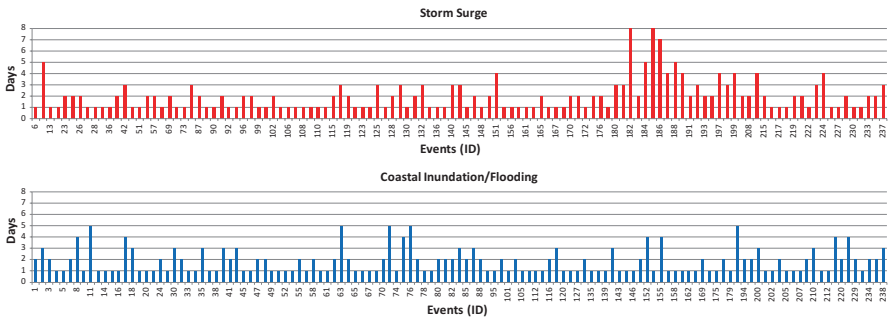

Fig. 6.6 Duration interval for storm surge and coastal inundation/flooding events

6.5.3 Lunar Phase

Figure 6.7 and Table 6.6 show that both types of events occurred during all lunar phases, including the intermediate phases, when the effects of one or the other are offset. However, most of the events occurred during the full moon (30.7%) and new moon (28.6%) phases, i.e. during spring tides, constituting 59.2% of the total (141 events).

For SS, the dominant phases are new moon (29.6%), waxing moon (23.5%) and full moon (22.6%), the spring tides predominating (52.2%). During the CI/F, as expected, full moon (38.2%) and new moon (27.6%) phases predominate, accounting for almost 66%.

However, the results show that factors other than the influence of the moon also contribute, since around 48% of SS events and 34% of CI/F occurred during neap tides and intermediate phases.

6.5.4 Meteorological Tide Heights

The meteorological tide heights varied from 0.01 to 0.78 m for both SS and CI/F (Fig. 6.8). The maximum height was reached in only one combined event, which occurred in 07 June 1985. Another seven events had meteorological tide heights ≥0.70 m (17 May 1977; 02 January 1980; 02 June 1988; 07 April 1997; 16 July 2000; 05 May 2001; 25 March 2003), four of them being combined events.

The overall average height for all the events (178 events with information) was 0.36 m; for SS, 0.35 m (84 events), and for CI/F, 0.38 m (94 events).

The predominant heights were 0.41–0.60 m, making up 36% of all events, 35.7% of the SS, and 36.2% of the CI/F (Table 6.7). For SS, that class was followed by the interval 0.01–0.20 m, in 34.5% of events. For CI/F, the second most frequent class was 0.21–0.40 m, in 31.9% of events. These results agree with those presented by Reguero et al. (2013) and CEPAL (2016), which found that the mean meteorological tide reaches 0.3–0.4 m at the São Paulo coast.

The monthly pattern of maximum meteorological tide heights (Fig. 6.9) show clearly the influence of the cyclone/storm surge season on both types of events, as expected. Only in January was the behaviour anomalous in relation to the summer

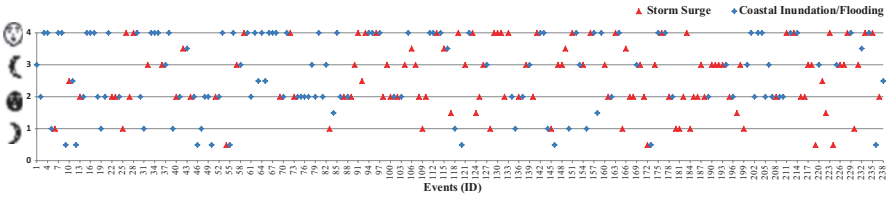

Fig. 6.7 Lunar phase

Table 6.6 Distribution of lunar phases

ALL			SS			CI/F		
Moon	**N° events**	**%**	**Moon**	**N° events**	**%**	**Moon**	**N° events**	**%**
0.5	16	6.7	**0.5**	5	4.3	**0.5**	11	8.9
1	23	9.7	**1**	13	11.3	**1**	10	8.1
1.5	3	1.3	**1.5**	2	1.7	**1.5**	1	0.8
2	68	28.6	**2**	34	29.6	**2**	34	27.6
2.5	7	2.9	**2.5**	3	2.6	**2.5**	4	3.3
3	40	16.8	**3**	27	23.5	**3**	13	10.6
3.5	8	3.4	**3.5**	5	4.3	**3.5**	3	2.4
4	73	30.7	**4**	26	22.6	**4**	47	38.2

See Table 6.1 and Fig. 6.9 above for lunar phase references
ALL all events (238), *SS* Storm Surge (115), *CI/F* Coastal Inundation/Flooding (123)

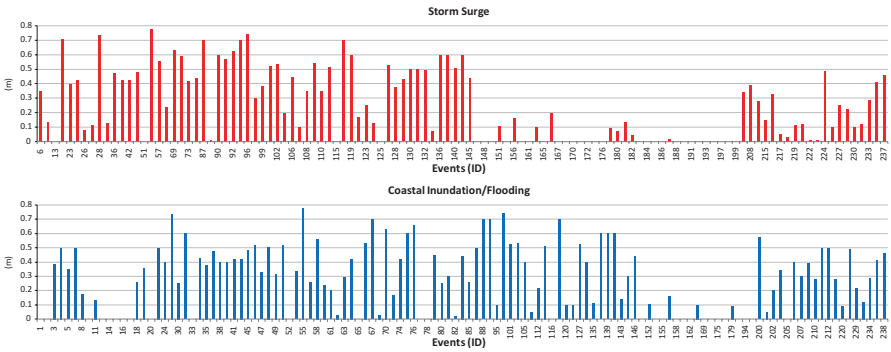

Fig. 6.8 Meteorological tide height for storm surge and coastal inundation/flooding events (the absence of bars signifies a gap in the data)

Table 6.7 Distribution of meteorological tides heights

Height	ALL		SS		CI/F	
Classes (m)	n°	%	n°	%	n°	%
0.01–0.20	50	28.1	29	34.5	21	22.3
0.21–0.40	46	25.8	16	19.0	30	31.9
0.41–0.60	64	36.0	30	35.7	34	36.2
0.61–0,78	18	10.1	9	10.7	9	9.6

months, due to the event of 02 January 1980 (0.73 m). The greatest meteorological tide height occurred in the month of June and corresponds to the combined event of 07 June 1985 (0.78 m). The month of May follows (0.74 m) with the combined event of 05 May 2001. The lowest heights occurred in December (0.44 m for CI/F and 0.28 m for SS).

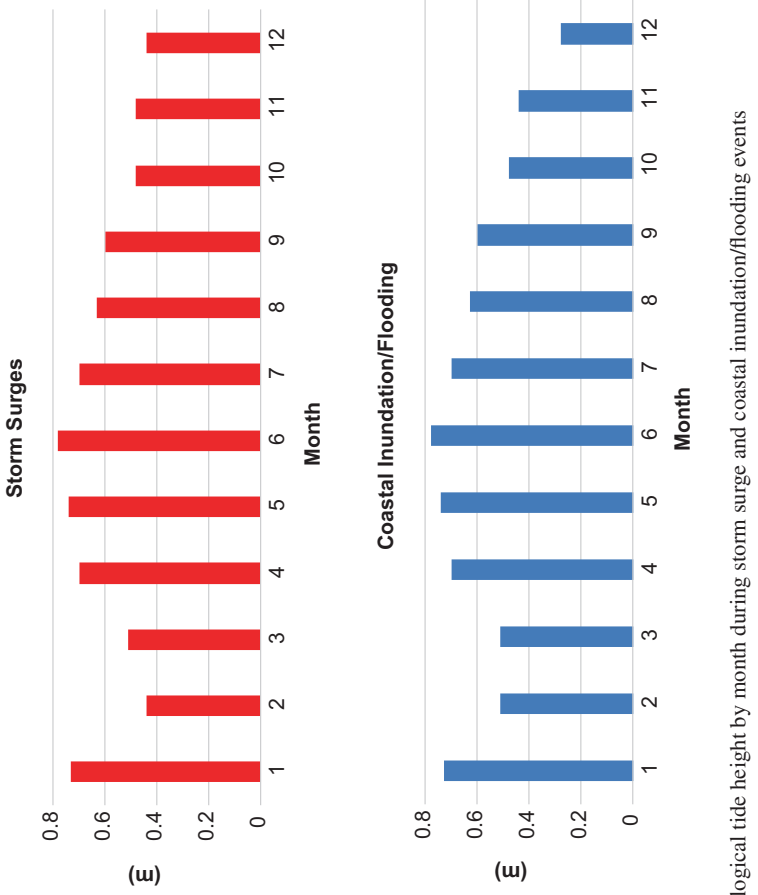

Fig. 6.9 Maximum meteorological tide height by month during storm surge and coastal inundation/flooding events

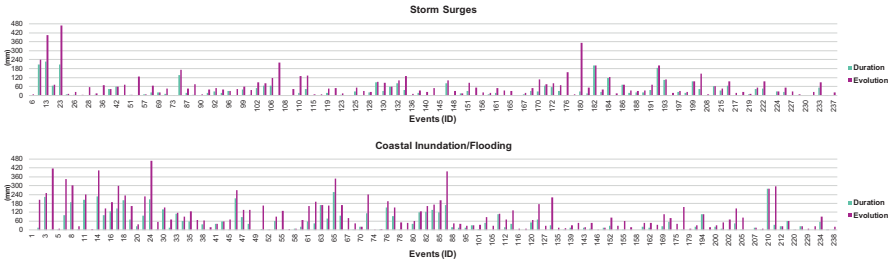

Fig. 6.10 Rainfall index distribution during duration interval and evolution period for storm surge and coastal inundation/flooding events

Table 6.8 Rainfall index classes for duration interval and evolution period of the events

	Rainfall	ALL (237)		SS (115)		CI/F (122)	
	Classes	n°	%	n°	%	n°	%
Duration interval	0–60	185	78.1	98	85.2	87	71.3
	61–120	29	12.3	13	11.3	16	13.1
	121–180	9	3.8	0	0,0	9	7.4
	181–240	11	4.6	5	4.3	7	5.7
	>240	3	1.3	0	0,0	2	1.6
Evolution period	0–100	172	72.6	96	83.5	76	62.3
	101–200	40	16.9	14	12.2	26	21.3
	201–300	15	6.3	3	2.6	12	9.8
	>300	10	4.2	3	2.6	7	5.7

6.5.5 Rainfall Volume

The pattern of rainfall accumulation in the event duration intervals and evolution periods are shown in Fig. 6.10.

For the event duration intervals, the greatest accumulations were 227.1 mm for SS and 277.8 mm for CI/F. For the evolution period, the greatest accumulation was 468.4 mm for both SS and CI/F.

Among all events, the average rainfall accumulation in the duration interval was 40.9 mm, and for the evolution period, 84.0 mm. In SS events, the averages were 33.1 mm for the duration interval and 63.9 mm for the evolution period. In CI/F events, the averages were 51.3 mm for the duration interval and 103.0 mm for the evolution period.

In the duration intervals of all events, the predominant rainfall accumulations were between 0 and 60 mm (78.1%), representing 85.2% of SS and 71.3% of CI/F events (Table 6.8). During the evolution period, rainfall accumulations between 0 and 100 mm occurred in 72.6% of events—83.5% of SS and 62.3% of CI/F.

These conclusions are also shown in the graphs of the monthly rainfall accumulation averages, which are controlled largely by seasonality (Fig. 6.11).

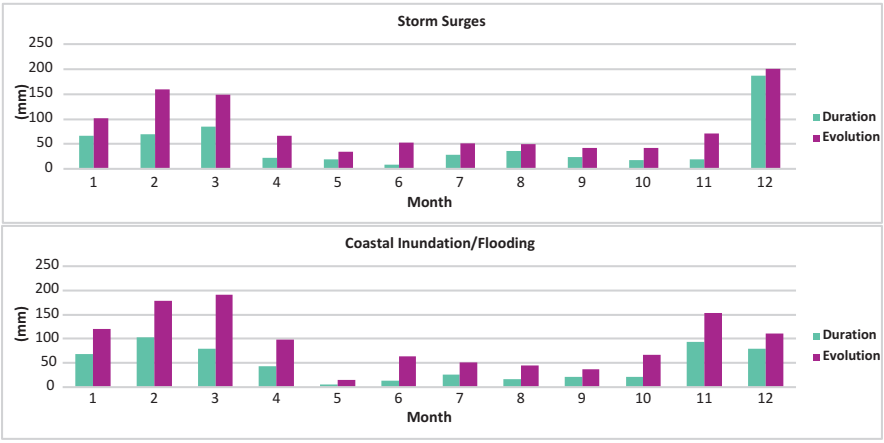

Fig. 6.11 Monthly distribution of mean rainfall index for storm surges and coastal inundation/flooding events

As expected, both types of events have the highest rainfall accumulations in the summer months (December to March). In the autumn/winter months (the SS season), lower accumulations prevail. For SS, the anomalous pattern in December is due to an isolated event (13 December 2010).

In the case of CI/F, seasonality clearly controls the type of process involved: in the spring/summer months (the rainiest), floods predominate, and during the cyclone season, the autumn/winter (least rainy), coastal inundations predominate.

The results also indicate a greater influence of rainfall on CI/F events than on SS events. This suggests low concomitance of a passing cold front and the peak of an SS event, which corroborates the studies of Campos et al. (2010).

6.5.6 Winds

The wind velocity varies between 1 (Light air) and 20.6 (Gale) m/s (Fig. 6.12). The average velocity for all 214 events was 6.63 m/s—for SS, 6.23 m/s, and for CI/F, 7.03 m/s; i.e., all were of the moderate Breeze class. The maximum velocities were 20.6 m/s (Gale) for SS and 17.0 m/s (near Gale) for CI/F.

In most events, the conditions were gentle to moderate Breeze (3.4–7.9 m/s), with very close distribution between the two classes, making up 73.4% of all events, 75.2% of the SS and 62.9% of the CI/F (Table 6.9). Winds between 8 and 20.6 m/s (fresh Breeze, strong Breeze, near Gale and Gale) occurred in 18.3% of SS and 32.4% of CI/F (though Gale winds did not occur during CI/F).

The results show predominant and average velocities slightly lower than those found by Campos et al. (2010), who concluded that during the events, winds near the coast are stronger than 8 m/s.

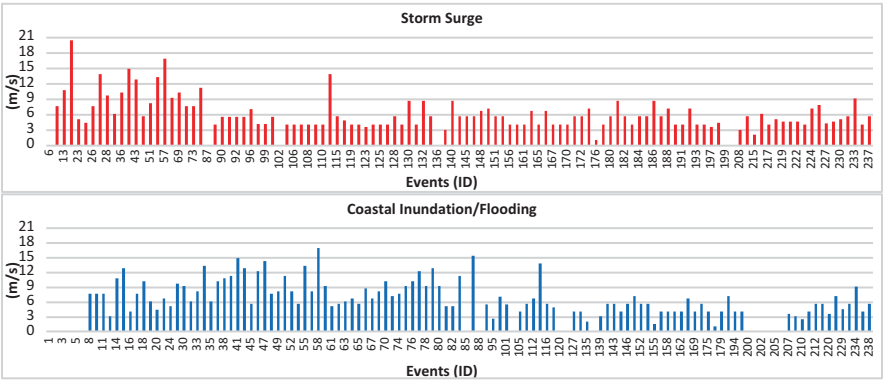

Fig. 6.12 Wind intensity for storm surge and coastal inundation/flooding events

Table 6.9 Wind intensity frequency according to the Beaufort scale

Beaufort scale (m/s)	Light air		Light breeze		Gentle breeze		Moderate breeze		Fresh breeze		Strong breeze		Near Gale		Gale	
	1–1.5		1.6–3.3		3.4–5.4		5.5–7.9		8–10.7		10.8–13-8		13.9–17.1		17.2–20.7	
Distribution	n°	%	n°	%	n°	%	n°	%	n°	%	n°	%	n°	%	n°	%
ALL	3	1.4	9	4.2	79	36.9	78	36.4	28	13.1	16	7.5	9	4.2	1	0.5
SS	1	0.9	6	5.5	42	38.5	40	36.7	11	10.1	4	3.7	4	3.7	1	0.9
CI/F	2	1.9	3	2.9	28	26.7	38	36.2	17	16.2	12	11.4	5	4.8	0	0.0

Regarding the wind direction (Fig. 6.13), values varied between 2° and 358° (N), the average of all events being 198° (SSW). During the SS events, winds varied between 2° and 358° (N), with an average of 204° (SSW). In CI/F, winds varied between 2° (N) and 340° (NNW), and the average was 191° (S-SSW).

The distribution of directions according to the classes and quadrants (Table 6.10) reveals a broad spectrum of winds blowing from all quadrants, notwithstanding a predominance of the S-W quadrant with similar percentages in all cases: 42.2% among all events, 42.3% among SS, and 42.1% among CI/F. These results corroborate the results of Campos et al. (2010).

SW (14.7%) and SSW (13.3%) were the predominant directions for all events as well as for CI/F (15% and 15.9%, respectively). For SS, SW (14.4%), S (12.6%) and WSW (12.6%) directions predominated.

6.5.7 Significant Waves

The significant wave heights (Hs) varied between 1 and 7 m (Fig. 6.14), the total average being 2.5 m (213 events). For SS, the average was 2.8 m (1.5–7 m; standard deviation 0.91), and for CI/F, 2.2 m (0.5–5.5 m; standard deviation 0.85).

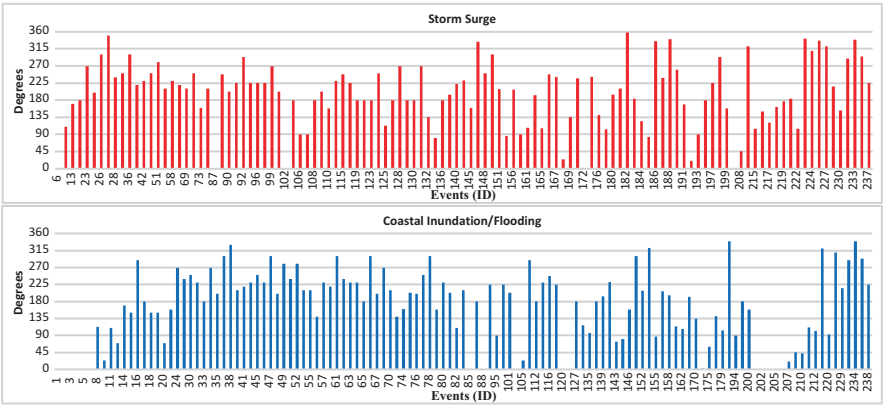

Fig. 6.13 Wind direction for storm surge and coastal inundation/flooding events

These results show heights greater than the mean annual Hs of 1.5 m obtained by Reguero et al. (2013) for the coast of São Paulo State.

The trend lines in both graphs suggest a slight increase in the Hs height over time. In the case of SS, if the purged value of event 22 (17 May 1977) were reduced, the slope of the line would increase considerably.

These trends agree with results from Reguero et al. (2013) and CEPAL (2016), which found increases in mean annual significant height (Hs) of ca. 6 mm/year; in Hs12, with mean values of around 3 cm/year; and in surge extremes, of 1.5 mm/year.

The distribution of significant wave height frequencies (Table 6.11) show that the intervals 1.1–2.0 and 2.1–3.0 m predominated in all situations, totalling 75.6% of all events, 70.3% of SS, and 81.4% of CI/F.

However, considering SS separately, the 2.1–3.0 m class (46.8%) predominated over the 1.1–2.0 m class (23.4%), contrary to CI/F, for which the 1.1–2.0 class (47.1%) predominated (as expected) over the 2.1–3.0 class (34.3%).

The next most frequent heights are 3.1–4.0 m, with 17.4% of the total; for SS, this class corresponds to 23.4%, same as the 1.1–2.0 m class. For the CI/F, as expected, the frequency is much lower, less than 11%.

No SS event had waves under 1.5 m, unlike the CI/F (nine events). Only seven events presented waves higher than 4 m, five of which were in SS (17 May 1977, 08 June 1981, 08 April 2010, 03 May 2011, 11 June 2016) and two in CI/F (08 June 1981, 03 May 2011). Note that two CI/F events were combined.

In relation to the monthly distributions of Hs (Fig. 6.15), the highest averages were concentrated in the autumn/winter months for both types of events, as expected, and varied between 2.6 m (September) and 3 m (May) during SS, and between 2.2 m (April) and 2.7 m (May/June) during CI/F. The month of November, however, fell outside this pattern, with averages of 3.1 m for SS and 3.3 m for CI/F. The lowest averages occurred in the summer months and December (2.3–2.7 m for SS and 1.7–2.1 m for CI/F).

Table 6.10 Frequency of wind directions

Quadrant	*N – E*				*E – S*				*S – W*				*W – N*		
(Degrees)	<36	36–55	56–80	81–100	101–120	121–145	146–170	171–190	191–210	211–235	236–260	261–280	281–310	311–335	>335
Direction	**N-NE**	**NE**	**NE-E**	**E**	**E SE**	**SE**	**SSE**	**S**	**SSW**	**SW**	**WSW**	**W**	**WNW**	**NW**	**NNW**
ALL (n°)	7	4	6	11	17	8	18	22	29	32	21	10	18	6	9
SS (n°)	3	1	1	6	8	4	9	14	12	16	14	5	8	3	7
CI/F (n°)	4	3	5	5	9	4	9	8	17	16	7	5	10	3	2
ALL (%)	12.8				29.8				42.2				15.1		
SS (%)	9.9				31.5				42.3				16.2		
CI/F (%)	15.9				28.0				42.1				14.0		

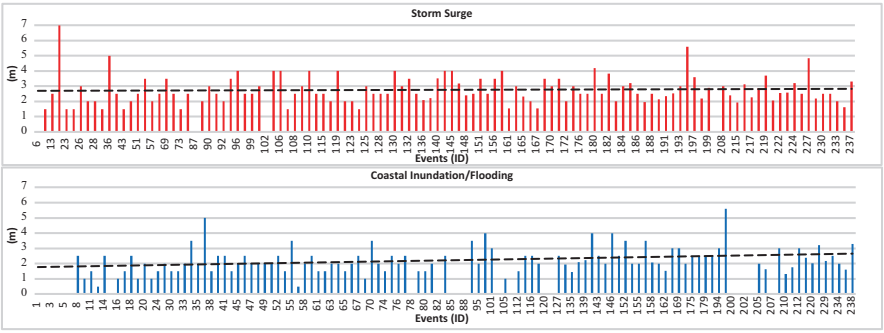

Fig. 6.14 Hs height for storm surge and coastal inundation/flooding events

Table 6.11 Frequency of significant waves (Hs) classes

Hs (m)	0.5–1.0		1.1–2.0		2.1–3.0		3.1–4.0		4.1–5.0		5.1–7.0	
Distribution	N°	%	N°	%	N°	%	N°	%	N°	%	N°	%
ALL	8	3.8	74	34.7	87	40.8	37	17.4	4	1.9	3	1.4
SS	0	0.0	26	23.4	52	46.8	26	23.4	3	2.7	2	1.8
CI/F	8	7.8	48	47.1	35	34.3	11	10.8	1	1.0	1	1.0

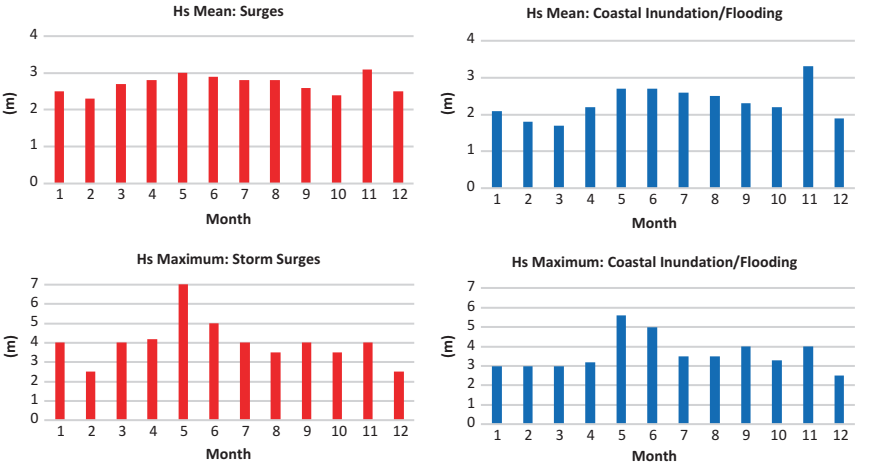

Fig. 6.15 Monthly mean and maximum Hs for storm surge and coastal inundation/flooding events

The pattern of maximum heights is less regular, though the month of May presented the greatest heights for both types of events (7 m for SS and 5.6 for CI/F), followed by the month of June (5 m for both). However, according to the studies of Reguero et al. (2013), these values obtained for May would be quite anomalous and

comparable to projections for the return periods of 50 years (5.5–6.0 m) and 500 years (7.0–8.0 m).

Regarding seasonality, the result obtained here, although from another sample universe, are similar to those in Reguero et al. (2013) (maximum mean Hs of 2.5 m for J-J-A, and 3.8 m for S-O-N)—for J-J-A, we found an overall average of 2.7 m and an average maximum of 4 m; for S-O-N, the overall average was 2.7 m, and the average maximum, 3.8 m; for combined events, the overall average was 2.7 m.

In relation to wave direction, note the more consistent behaviour in the SS events than in CI/F events (Fig. 6.16). The directions varied between 23° (NNE) and 300° (NW), the average among all events being 170° (SSE-S). During SS, waves varied from 90° (E) to 300° (NW), with an average of 177° (S). During CI/F, the direction varied from 23° (NNE) to 280° (W), with an average of 162° (SSE).

The distribution of directions according to classes and quadrants reveal that waves originate mainly from the E-S quadrant, with similar percentages in all cases: 70.7% among all events, 75.5% during SS, and 65.7% during CI/F (Table 6.12).

The predominant direction was S, followed by SSE, with the following distribution, respectively: 34.4% and 21.4% in relation to all events; 41.8% and 25.5% for SS; and 26.7% and 17.1% for CI/F.

6.5.8 El Niño and La Niña

Among the 238 registered events, 212 (89.1%) occurred in phases of ENSO activity, 50.4% of them under El Niño (EN) and 38.7% during La Niña (LN) (Table 6.13).

Most of the events happened during phases of moderate to weak EN (37.8%) and moderate to weak LN (33.6%); the phases of strong/very strong EN/LN totalled 17.6% of all events. Thus, only 10.9% of the events occurred in phases of neutrality.

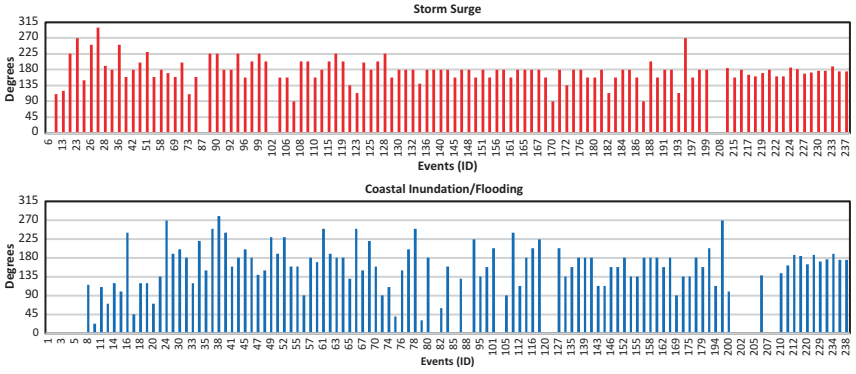

Fig. 6.16 Hs direction for storm surge and coastal inundation/flooding events

Table 6.12 Frequency of Hs directions

Quadrant	*N – E*				*E – S*				*S – W*				*W – N*
(Degrees)	<36	36–55	56–80	81–100	101–120	121–145	146–170	171–190	191–210	211–235	236–260	261–280	281–305
Direction	N-NE	NE	NE-E	E	ESE	SE	SSE	S	SSW	SW	WSW	W	WNW
ALL (n°)	1	3	3	9	17	15	46	74	18	14	9	5	1
SS (n°)	0	0	0	3	6	3	28	46	11	8	2	2	1
CI/F (n°)	1	3	3	6	11	12	18	28	7	6	7	3	0
ALL (%)	7.4				70.7				21.4				0.5
SS (%)	2.7				75.5				20.9				0.9
CI/F (%)	12.4				65.7				21.9				0.0

Table 6.13 Frequency of ENSO phases and intensities

Events	Intensity / Distribution	Strong/very strong n°	Strong/very strong %	Moderate n°	Moderate %	Weak n°	Weak %	Total n°	Total %
ALL	El Niño	30	12.6	46	19.3	44	18.5	120	50.4
	La Niña	12	5.0	40	16.8	40	16.8	92	38.7
	Neutrality							26	10.9
SS	El Niño	16	13.9	24	20.9	23	20,0	63	54.8
	La Niña	2	1.7	25	21.7	19	16.5	46	40.0
	Neutrality							6	5.2
CI/F	El Niño	14	11.4	22	17.9	21	17.1	57	46.3
	La Niña	10	8.1	15	12.2	21	17.1	46	37.4
	Neutrality							20	16.3

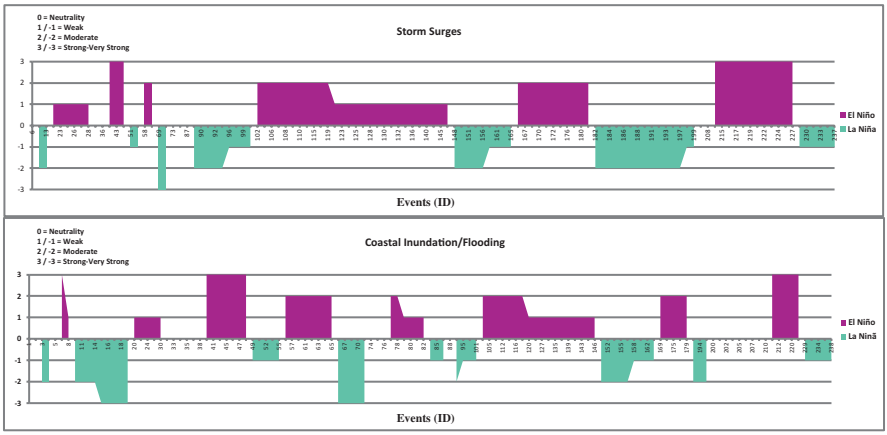

Fig. 6.17 ENSO phases and intensities for storm surge and coastal inundation/flooding events

SS events had the following distribution: 54.8% under EN activity, moderate and weak intensities predominating, with similar percentages of about 20% each; 40% of events happened during LN, with predominantly moderate intensity (21.7%); only 5.2% of the events occurred during neutrality phases.

For CI/F events, the trends were somewhat similar: 46.3% occurred under EN activity, with predominantly moderate to weak intensities and similar percentages of around 17% each; 37.4% of the events happened in LN, with predominantly weak intensity (17.1%); and during the neutrality phases, 16.3% of the events occurred.

The temporal distribution of the events, illustrated in the graphs of Figs. 6.17 and 6.18, show the increasing trend in the number of events with EN and LN activity, starting in the 2000s.

When compared to the years of global ENSO occurrence (see, for example: http://ggweather.com/enso/oni.htm), these results underline the conditioning of the

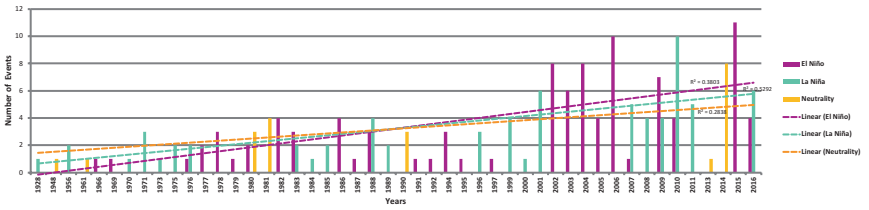

Fig. 6.18 ENSO and neutrality phases in an annual distribution of SS and CI/F events (conjugated events of SS and CI/F were considered as only 1 event)

extreme climatic events at the global scale, but they also suggest that other factors must be controlling these events, among them the regional climatic variability and the behaviour of the atmospheric systems preceding ENSO itself, as well as other possible forcings not analysed here.

However, as seen in Table 6.13, the intensity of the ENSO does not seem to influence the number of events per year, because in the years with strong El Niño and La Niña activity, the number of events did not increase, with exception of 2015–2016; however, these years still follow the decadal trend.

The control exerted by other forcings is clear when the following are observed: (a) the occurrence of 26 events (10.9%) during neutrality phases, 20 CI/F and 6 SS, and distributed throughout all seasons of the year; (b) the reduced number of events in the 1950s and 1960s, because, since the 1950s at least, the number of years with global ENSO seems not to have varied much (8 in the 1950s, 6 in the 1960s, 1980s, 1990s e 2000s, 9 in the 1970s, and 4 between 2011 and 2016); (c) there is no apparent link between El Niño–Southern Oscillation (ENSO/SOI) and wave climate in the South Atlantic coast, either for wave heights or for directions, as postulated by Reguero et al. (2013).

6.6 Final Remarks

The volume of manipulated data in the database exceeded 7000.

A synthesis of the main conditions surrounding the 238 events is exhibited in Table 6.14.

The two events considered most intense, given the proportion of their impacts on the Santos coastline, were combined; their characteristics are presented in Table 6.15. It is interesting to note that neither of them presented very high Hs, meteorological tide or wind intensity values.

This and all the results presented here suggest that, as mentioned previously, other factors are also very important triggers of impacts on Santos. One of the main factors must be the direction of the waves entering the Bay of Santos and the changes they undergo until they reach the coastline. The local winds, in turn, can also affect the behaviour of these waves and of the longshore drift currents during extreme

Table 6.14 Summary of the boundary conditions for SS and CI/F events

Indicator	Storm Surge (115 events)	Coastal Inundation/Flooding (123 events)
Distribution	Highest n° of events: 2000s (49 = 42.6%); year 2010 (14); 33% in May and July; 76.5% between April and September	Highest n° of events: 2000s (34 = 27.6%); years 2006 and 2014 (8 each); 16.3% in March; 50.4% between January and April
	21st century (2000–2016): 76.5% of the total; increased by 3.3 times relative to the 20th century	21st century: 47.2% of the total; reduction by 0.9 or constant relative to the 20th century
Duration	Average: 1.9 days (1–8 days)	Average: 1.8 days (1–5 days)
Lunar phase	52.2%: during spring tides	65.6% during spring tides
	34.8%: during neap tides	18.7%: during neap tides
Meteorological tide height	Average 0.35 m (maximum: 0.78 m); predominant 0.41–0.60 m (35.7%); greatest heights (>0.7 m) in January, May and June	Average 0.38 m (maximum: 0.78 m); predominant 0.41–0.60 m (36.2%); greatest heights (>0.7 m) in January, May and June
Rainfall volume	Duration interval: average 33.1 mm; maximum 227.1 mm; 0–60 mm accumulated = 84.3%	Duration interval: average 51.3 mm; maximum 277.8 mm; 0–60 mm accumulated = 72.1%
	Evolution period: average 63.9 mm; maximum 468.4 mm; 0–100 mm accumulated = 83.5%	Evolution period: average 103.0 mm; maximum 468.4 mm; 0–100 mm accumulated = 62.3%
Winds	Intensity: average 6.2 m/s (moderate breeze); maximum 20.6 m/s (gale); 75.2% between 3.4 and 7.9 m/s (gentle-moderate breeze)	Intensity: average 7.0 m/s (moderate breeze); maximum 17.0 m/s (near gale); 62.9% between 3.4 and 7.9 m/s (gentle-moderate breeze)
	Direction: average 204° (SSW) (2–358°); SW/S/WSW predominate (37.8%)	Direction: average 191° (S-SSW) (2–340°); SW/SSW predominate (30.9%)
Significant Waves	Height: average 2.8 m; maximum 7 m; 75.7% between 1.5 and 3.0 m; 45% between 2.5 and 3.0 m; highest average in May (3.0 m)	Height: average 2.2 m; maximum 5.5 m; 80.4% between 1.5 and 3.0 m; 50% between 1.5 and 2.0 m; highest average in May–June (2.7 m)
	Direction: average 177° (S) (90–300°); S/SSE predominate (41.8 and 25.5%)	Direction: average 162° (SSE) (23–280°); S/SSE predominate (26.7 and 17.1%)
ENSO	El Niño: 54.8%; moderate to weak intensities predominate (40.9%)	El Niño: 46.3%; moderate to weak intensities predominate (35%)
	La Niña: 40%; moderate intensity predominates (21.7%)	La Niña: 37.4%; weak intensity predominantes (17.1%)
	Neutrality: 5.2%	Neutrality: 16.3%

events. Furthermore, the morphodynamic state of the beach preceding an extreme event is also a determinant of how the beach receives and readjusts to the impacts of storm waves. Beaches in a state of chronic erosion and beaches affected by consecutive SS (acute erosion) will present morphodynamic disequilibrium and negative

Table 6.15 Characteristics of the most impactful events for Santos coastline

Date	Duration (day)	Lunar phase	Meteorological tide (m)	Rainfall volume: event duration; evolution period (mm)	Winds: intensity; direction	Significant Waves: height direction	ENSO
26/04/2005	1	Full	0.50	26.6; 85.4	8.7 m/s; 180º	4.0 m; 180º	Weak EN
27/04/2016	4	Full/ waning	0.49	26.4; 26.4	7.2 m/s; 310º	3.2 m; 187º	Strong EN

sedimentary balance, which will result in greater erosion during SS, facilitating the incursion of water over the mainland and increasing coastal inundation.

Therefore, there is clearly a need to gather local monitoring data to better understand the behaviour of these very complex extreme events.

In any respect, the data set obtained for this 89-year historical series of extreme events of SS and CI/F in the Baixada Santista region, today constitutes an important tool for the municipal contingency[1] plans for storm surges and anomalous high tides (currently under development in most cases) as well as city planning within the context of climate change and its effects.

Although the socioeconomic impacts caused by these events are difficult to quantify, the damages and restoration expenses in many cases were on the order of millions of Brazilian reals, especially after large-magnitude events.

Acknowledgements The authors thank Oceanographer Eduardo G. Rosa, Environmental Analyst Johann C. Lima and Geographer Graziella S. R. Rodrigues for conducting part of the work of compiling the data and making some graphic treating. We also thank Dr. Mirian R. Gutjahr (Instutute of Geology-SMA/SP) and Professor Dr. Luci H. Nunes (LECLIG-University of Campinas) for making available their disaster registries for São Paulo coastal zone; the BNDO – National Bank of Oceanographic Data (Captain Vladimir C. Maluf in particular), the Centre for Hydrodynamic Research at the University Santa Cecília (Profs. Renan B. Ribeiro MSc. and Dr. Alexandra F. P. Sampaio), as well as the Santos Civil Defence (Eng. Ernesto K. Tabuchi and Geologist Marcos P. Bandini in particular) for kindly making their databases available. Finally, our thanks to the State of São Paulo Docas Company (2010–2011), the IG-SMA/SP, and the São Paulo Research Foundation (Fapesp n° 2012/51876-0 and 2015/08192-1) for the various types of financial support for this research.

[1] In 2016, São Paulo State created the "*Plano Preventivo de Defesa Civil para Erosão Costeira, Inundações Costeiras e Enchentes/Alagamentos causadas por Eventos Meteorológicos-Oceanográficos Extremos como Ressacas do Mar e Marés Altas*" (a preventative plan for coastal erosion, coastal inundation and flooding caused by meteorological-oceanographic extremes such as storm surges and high tides), in which one of the main instruments is the municipal contingency plan, *Plano Municipal de Contingência* (*Resolução CMIL 17-610 – Cedec, de 28-11-2016*).

References

Bittencourt, A. C. S. P., Medeiros, K. O. P., Dominguez, J. M. L., Guimarães, J. K., & Dutra, F. R. L. S. (2008). Severe coastal erosion hotspots in the city of Salvador, Bahia, Brazil. *Shore and Beach, 76*, 8–14.

Camargo, R., & Harari, J. (1994). Modelagem numérica de ressacas na plataforma sudeste do Brasil a partir de cartas sinóticas de pressão atmosférica na superfície. *Boletim do Instituto Oceanográfico USP, 42*(1), 19–34.

Campos, R. M., Camargo, R., & Harari, J. (2010). Caracterização de eventos extremos do nível do mar em Santos e sua correspondência com as re-análises do modelo do NCEP no Sudoeste do Atlântico Sul. *Revista Brasileira de Meteorologia, 25*, 175–184.

CEPAL-Comisión Económica para America Latina y el Caribe. (2016). *Efectos del cambio climático en la costa de América Latina y el Caribe: Dinámicas, tendencias y variabilidad climática*. Santiago de Chile: Naciones Unidas. Available https://www.cepal.org/es/publicaciones/3955-efectos-cambio-climatico-la-costa-america-latina-caribe-dinamicas-tendencias. Accessed May 2017.

Gan, M. A., & Rao, B. V. (1991). Surface ciclogenesis over South America. *Monthly Weather Review, 119*, 293–302.

Gasparro, M. R., Sousa, E. C. P. M., Giordano, F., Argentino-Santos, R. C. (2008). *Occupation history of the Santos estuary, perspectives on integrated coastal zone management in South America*. In: R. Neves, et al. (Eds.), IST Press. Available https://www.unisanta.br/arquivos/CoastalZoneManagementFinal.pdf. Accessed May 2017.

Gutjahr, M. R. (coord) (2011). *Banco de Dados: Estudos históricos relacionados a eventos climáticos na Baixada Santista – SP*. Instituto Geológico–SMA/SP. Available http://www.igeologico.sp.gov.br. Accessed May 2010.

IPCC-Intergovernmental Panel on Climate Change. (2012). Managing the risks of extreme events and disasters to advance climate change adaptation. In C. B. Field et al. (Eds.), *Special report of working groups I and II of the Intergovernmental Panel on Climate Change*. Cambridge: Cambridge University Press. Available https://www.ipcc.ch/pdf/special-reports/srex/SREX_Full_Report.pdf. Accessed May 2017.

IPCC-Intergovernmental Panel on Climate Change. (2014). Summary for policymakers. In C. B. Field et al. (Eds.), *Climate change 2014: impacts, adaptation and vulnerability. Part A: Global and sectoral aspects. Contribution of working group II to the fifth Assessment report of the Intergovernmental Panel on Climate Change*. Cambridge: Cambridge University Press. Available https://www.ipcc.ch/pdf/assessment-report/ar5/wg2/ar5_wgII_spm_en.pdf. Accessed May 2017.

Lins-de-Barros, F. M. (2010). *Contribuição metodológica para análise local da vulnerabilidade costeira e riscos associados: Estudo de caso da Região dos Lagos*. Tese de Doutorado: Universidade Federal do Rio de Janeiro.

Losada Rodríguez, I. J., Reguero, B. G., Méndez, F. J., Castanedo, S., Abascal, A. J., & Mínguez, R. (2013). Long-term changes in sea-level components in Latin America and the Caribbean. *Global and Planetary Change, 104*, 34–50.

Machado, A. A., Calliari, L. J., Melo, E., & Klein, A. H. F. (2010). Historical assessment of extreme coastal sea state conditions in southern Brazil and their relation to erosion episodes. *Pan-American Journal of Aquatic Sciences, 5*(2), 277–286.

Magrin, G. O., Marengo, J. A., Boulanger, J. P., Buckeridge, M. S., Castellanos, E., Poveda, G., Scarano, F. R., & Vicuña, S. (2014). Central and South America. In V. R. Barros et al. (Eds.), *Climate change: Impacts, adaptation, and vulnerability. Part B: Regional aspects*, *Contribution of working group ii to the fifth Assessment report of the Intergovernmental Panel on Climate Change* (pp. 1499–1566). Cambridge: Cambridge University Press. Available https://www.ipcc.ch/pdf/assessment-report/ar5/wg2/WGIIAR5-Chap27_FINAL.pdf. Acessed May 2017.

Mangor, K., Drønen, N. K., Kærgaard, K. H., & Kristensen, S. E. (2017). *Shoreline management guidelines* (4ª ed.). Horsholm: DHI Water & Environement. Available https://www.dhigroup.

com/upload/campaigns/shoreline/assets/ShorelineManagementGuidelines_Feb2017-TOC.pdf. Accessed May 2017.

Marengo, J. A., Scarano, F. R., Klein, A. F., Souza, C. R. G., & Chou, S. C. (2017a). Impacto, vulnerabilidade e adaptação das cidades costeiras brasileiras às mudanças climáticas. In J. A. Marengo & F. R. Scarano (Eds.), *Relatório especial do Painel Brasileiro de Mudanças Climáticas (PBMC)*. Rio de Janeiro: COPPE-UFRJ. https://doi.org/10.13140/RG.2.2.36042.16329.

Marengo, J. A., Nunes, L. H., CRG, S., Harari, J., Hozokawa, E. K., & Tabuchi, E. K. (2017b). Vulnerability in Brasilian coastal comunities: An integrated framework to analyse local decision making and adaptation to sea-level rise in Santos, São Paulo – Brazil. In V. Marchezini et al. (Eds.), *Redution of vulnerability to disasters: From knowlegde to action* (Vol. 1, 1st ed., pp. 397–408). São Carlos: Rima Editora.

Marone, E., & Camargo, R. (1994). Marés meteorológicas no litoral de estado do Paraná: o evento de 18 de agosto de 1993. *Revista Nerítica, 8*(1–2), 73–85.

Muehe, D. (org) (2006). *Erosão e progradação do litoral brasileiro*. MMA/PGGM, Brasília, DF, p 476.

Nicholls, R. J. (2006). Storm surges in coastal areas. In M. Arnold et al. (Eds.), *Natural disaster hotspots – case studies*, *Disaster Risk Management Ser nº 6* (pp. 79–108). Washington, DC: The World Bank Hazard Management Unit.

NOAA-National Oceanic and Atmospheric Administration. (2017). *What is storm surge*? Available https://oceanservice.noaa.gov/facts/stormsurge-stormtide.html. Accessed May 2017.

Parise, C. K., Calliari, L. J., & Krusche, N. (2009). Extreme storm surges in the south of Brazil: atmospheric conditions and shore erosion. *Brazilian Journal of Oceanography, 57*(3), 175–188.

Paula, D. P., Morais, J. O., Ferreira, O., & Dias, J. A. (2015). *Análise histórica das ressacas do mar em Fortaleza (Ceará, Brasil): origem, características e impactos*. In: D. V. Paula, & J. A. Dias (orgs) Ressacas do mar/temporais e gestão costeira, pp 173–201.

PBMC-Painel Brasileiro de Mudanças Climáticas. (2014). Base científica das mudanças climáticas. In T. Ambrizzi & M. Araújo (Eds.), *Contribuição do grupo de trabalho 1 do Painel Brasileiro de Mudanças Climáticas ao primeiro Relatório da avaliação nacional sobre mudanças climáticas* (p. 464). Rio de Janeiro: COPPE, Universidade Federal do Rio de Janeiro.

Pontes, N. Z., & Zee, D. M. W. (2010). *Mudanças climáticas globais e seus reflexos nas praias oceânicas do município do Rio de Janeiro*. In: Expanded Abstracts of the 4° Congresso Brasileiro de Oceanografia, Rio Grande, RS, October 2010.

Pugh, D. T. (1987). *Tides, surges and mean sea level. A handbook for engineers and scientists* (p. 472). New York: Wiley.

Reboita, M. S., Rocha, R. P., & Ambrizzi, T. (2010). South Atlantic ocean cyclogenesis climatology simulated by regional climate model (RegCM3). *Climate Dynamics, 35*, 1331–1347.

Reguero, B. G., Méndez, F. J., & Losada, I. J. (2013). Variability of multivariate wave climate in Latin America and the Caribbean. *Global and Planetary Change, 100*, 70–84.

Ribeiro, R. B., Leitão, J. M. C. F. L., Leitão, P. M. C. F. L., Puia, H. L., & Sampaio, A. F. P. (2016). *Integration of high-resolution metocean forecast and observing systems at Port of Santos*. In: Proceedings of the IX PIANC-COPEDEC, Conference on Coastal and Port Engineering in Developing Countries, Rio de Janeiro, October 2016.

Rudorff, F. M., Bonetti Filho, J., Moreno, D. A., Oliveira, C. A. F., & Murara, P. G. (2014). Maré de tempestade. In M. L. P. Herrmann (Ed.), *Atlas de Desastres Naturais do Estado de Santa Catarina: Período de 1980 a 2010* (pp. 151–154). Florianópolis, Santa Catarina, Brasil: Cadernos Geográficos.

Santana, C. L., Souza, C. R. G., & Harari, J. (2004). *Correlação de dados pluviométricos, fluviométricos e maregráficos em eventos de enchentes/inundações no baixo Rio Ribeira de Iguape (SP)*. In: Proceedings of the I Simpósio Brasileiro de Desastres Naturais – SIBRADEN, Florianópolis, September 2004.

Satyamurti, P., Nobre, C., & Dias, P. L. S. (1998). South America. In D. J. Karoly & D. J. Vincent (Eds.), *Meteorology of the Southern Hemisphere* (pp. 119–139). Boston: American Meteorological Society.

Sinclair, M. R. (1996). A climatology of anticyclones and blocking for the Southern Hemisphere. *Monthly Weather Review, 124*, 245–264.

Souza, C. R. G. (2009a). A erosão costeira e os desafios da gestão costeira no Brasil. *J Integr Coast Manag, 9*, 17–37.

Souza, C. R. G. (2009b). *A erosão nas praias do estado São Paulo: causas, consequências, indicadores de monitoramento e risco*. In: Bononi VLR, Santos Júnior NA (org) Memórias do conselho científico da Secretaria do Meio Ambiente: A síntese de um ano de conhecimento acumulado. Instituto de Botânica-SMA/SP, São Paulo, pp 48–69.

Souza, C. R. G. (2009c). Flood risk assessment in coastal drainage basins through a multivariate analysis within a GIS-based model. *Journal of Coastal Research, SI, 56*(1), 900–904.

Souza, C. R. G. (2010). *Impactos das mudanças climáticas no litoral do Estado de São Paulo (Sudeste do Brasil)*. In: Proceedings of the VI Seminário Latino Americano de Geografia Física e II Seminário Ibero Americano de Geografia Física, Coimbra. Available http://www.uc.pt/fluc/cegot/VISLAGF/actas/tema4/celia_regina. Accessed May 2107.

Souza, C. R. G. (2011). *Os ecossistemas costeiros frente às mudanças climáticas no Brasil: efeitos da elevação do nível do mar*. In: Expanded abstracts of the XIV Congresso Latino-Americano de Ciências do Mar – COLACMAR, Balneário Camboriú, October–November 2011.

Souza, C. R. G. (2012). Oceanic sandy beaches of São Paulo (Brazil): Synthesis of knowledge on morphodynamics, sedimentology, sediment transport and coastal erosion. *J Dep Geogr USP*, n. 2012, Spec Vol 30 yers, pp 308–371. https://doi.org/10.7154/RDG.2012.0112.0015.

Souza, C. R. G. (2017). Balanço sedimentar de longo e curto termos da Praia de Santos e causas da erosão na Ponta da Praia. In: Proceedings of XVI Congresso Associação Brasileira de Estudos do Qaternário (ABEQUA), Bertioga (São Paulo), 21–27/10/2017. http://www.abequa.org.br/trabalhos/254_resumo.PDF. (ISSN: 2318–0986). Accessed May 2017.

Souza, C. R. G., Souza Filho, P. W. M., Esteves, S. L., Vital, H., Dillemburg, S. R., Patchineelam, S. M., & Addad, J. E. (2005). Sandy beaches and coastal erosion. In Souza et al. (Eds.), *Quaternário do Brasil* (pp. 130–152). Ribeirão Preto: Holos Editora.

Souza, C. R. G., Luna, G. C., & Souza, A. P. (2012). *Causas da erosão na Ponta da Praia de Santos (São Paulo, Brasil)*. In: Abstracts of the II Workshop Antropicosta Iberoamerica, Montevideo, 2012.

Souza, C. R. G., Gouveia, M. L., & Souza, A. P. (2016a). *Balanço sedimentar da Praia de Santos antes, durante e após as obras de dragagem de aprofundamento do canal do Porto de Santos (São Paulo, Brasil)*. In: Abstracts of the VII Congresso Latinoamericano de Sedimentologia and XV Reunión Argentina de Sedimentologia, Santa Rosa, October 2012. Available http://www.isbn.org.ar/cal/laimg/21314/488040.pdf. Accessed May 2017.

Souza, C. R. G., Souza, A. P., & Gouveia, M. L. (2016b). *Identificação de processos sedimentares em praias por meio da variabilidade temporal de células de deriva litorânea*. In: Abstracts of the VII Congresso Latinoamericano de Sedimentologia and XV Reunión Argentina de Sedimentologia, Santa Rosa, October 2012. http://www.isbn.org.ar/cal/laimg/21314/488040.pdf. Accessed May 2017.